Proc. of the 13th Symposium of Magnetic Measurements and Modeling SMMM'2018, Wieliczka, Poland, October 8–10, 2018

Magnetic Properties of the Rapidly Solidified $Gd_3Zr_{10}Fe_{55}Co_{10}Mo_5W_2B_{15}$ Alloy

K. Kotynia[a,*], A. Chrobak[b] and P. Pawlik[a]

[a]Institute of Physics, Częstochowa University of Technology, Al. Armii Krajowej 19, 42-200 Częstochowa, Poland
[b]Institute of Materials Science, University of Silesia, 75 Pułku Piechoty 1, 41-500 Chorzów, Poland

Studies of magnetic properties for the $Gd_3Zr_{10}Fe_{55}Co_{10}Mo_5W_2B_{15}$ glassy alloy are presented. The amorphous structure of melt-spun ribbon of investigated alloy was confirmed by X-ray diffractometry. The Curie temperature T_C was determined analyzing $M(H)$ dependences measured at various temperatures as well as from $M(T)$ dependence measured at low constant magnetic field. Furthermore, the isothermal magnetic entropy changes $|-\Delta S_M|$ were calculated from the magnetization curves to assess the possibility of potential application of studied samples as active elements in magnetic refrigerators.

DOI: 10.12693/APhysPolA.136.696

PACS/topics: 78.55.Qr, 71.20.Eh, 75.50.Bb, 75.50.Kj

1. Introduction

The growing interest in magnetocaloric materials was caused by using them in cooling systems operating near room temperature. Moreover, in recent years, the magnetocaloric effect was also used in the power industry to convert industrial waste heat to electricity [1]. There are three physical quantities that designate the usefulness of magnetocaloric materials: the magnetic entropy change $|-\Delta S_M|$, the adiabatic temperature change $|-\Delta T_{ad}|$, and the relative cooling power (RCP) [2]. An ideal magnetic refrigerant material should exhibit large values of both $|-\Delta S_M|$ and $|-\Delta T_{ad}|$, as well as high RCP around room temperature at the low magnetic field [3]. High magnetic entropy change was found in $Gd_5(Si_2Ge_2)$ [4], MnAs [5], and MnFe(P,As) alloys [6]. The first order magnetostructural phase transition and the appearance of hysteretic losses were observed for these alloys. Although these materials reveal significant $|-\Delta S_M|$ and $|-\Delta T_{ad}|$ their major drawbacks are low RCP and complex processing route. Despite relatively low $|-\Delta S_M|$ and $|-\Delta T_{ad}|$ values, due to second order magnetic phase transition, the amorphous alloys seems to be an interesting alternative for their large RCP and low processing costs.

Until now we have performed studies of the magnetocaloric effect for $Gd_xZr_{10}Fe_{58-x}Co_{10}Mo_5W_2B_{15}$ (where x = 0, 1, 2, 3, 4, 5 at.%), that have shown good glass forming abilities for all investigated compositions [7]. Furthermore, increase in Gd contents resulted in the increase of the Curie temperature of amorphous phase [8]. Besides, in all cases a broad $|-\Delta S_M|$ peak around T_C was observed [8–10]. Therefore the aim of the present work was to investigate the influence of further admixture of Gd on structural and magnetocaloric properties of the $Gd_3Zr_{10}Fe_{55}Co_{10}Mo_5W_2B_{15}$ alloy.

2. Sample preparation and experimental methods

The $Gd_3Zr_{10}Fe_{55}Co_{10}Mo_5W_2B_{15}$ alloy was obtained by the arc-melting of the high purity (99.98%) constituent elements Gd, Zr, Fe, Co, Mo, W with the addition of pre-alloyed Fe–B. Alloy composition represents nominal atomic percentage. To protect oxidation during melting the titanium was used as a getter. The ingot was re-melted seven times to guarantee a homogeneity of the alloy.

The ribbon was prepared by the melt-spinning technique at a surface velocity of the copper roll of 32 m/s. Both the arc-melting and melt-spinning techniques were performed under an Ar atmosphere to avoid oxidation.

The phase structure was investigated by the X-ray diffractometry (XRD) using the Bruker D8 Advance diffractometer with Cu K_α radiation and the LynxEye detector. The data were recorded using the Bragg–Brentano continuous-scan method in $2\Theta p$ range between 30 and 100 degrees.

The field dependences of magnetization were recorded in the field cooling mode (FC) by SQUID MPMS XL-7 Quantum Design system. The magnetic measurements $M(H)$ were performed in the temperature range between 150 K and 350 K. Based on those results the Arrott plots were constructed. Magnetocaloric effect MCE was estimated by calculation of the temperature dependences of magnetic entropy change $|-\Delta S_M|$ for various changes of external magnetic fields according to the Maxwell thermodynamic formula [11]:

$$\Delta S_M(TH) = \int_0^H \left(\frac{\partial M(T,H)}{\partial T}\right)_H \mathrm{d}H, \tag{1}$$

where T is temperature, $M(T,H)$ is magnetization, H is external magnetic field.

*corresponding author; e-mail: k.kotynia@po.edu.pl

3. Results

X-ray diffraction pattern measured for the melt-spun ribbon of the $Gd_3Zr_{10}Fe_{55}Co_{10}Mo_5W_2B_{15}$ alloy is shown in Fig. 1.

A broad peak between $2\Theta = 30$ deg and 50 deg suggests amorphous structure of the rapidly solidified ribbon.

One of the most important parameters which facilitates the potential applicability of a material in the magnetic refrigeration is the Curie temperature T_C. In order to determine T_C we have used four methods described below.

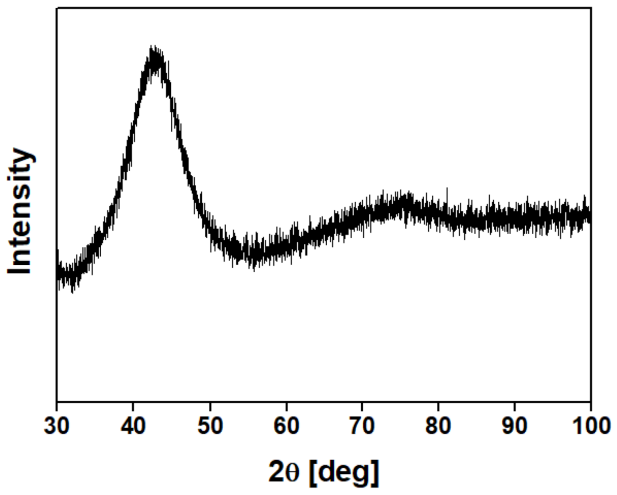

Fig. 1. XRD pattern measured for melt-spun ribbon of the $Gd_3Zr_{10}Fe_{55}Co_{10}Mo_5W_2B_{15}$ alloy.

3.1. Determination of T_C from dM/dT dependence

The temperature dependence of magnetization was shown in Fig. 2.

The $M(T)$ curve is typical for the amorphous materials. The magnetization gradually decreases with the increase of temperature around T_C. For this purpose the dM/dT derivative was calculated and T_C reaching 316 K was determined as a temperature corresponding to the minimum value of dM/dT.

3.2. Determination of T_C using critical exponent in Heisenberg model

In amorphous alloys the change of magnetization around the Curie temperature proceeds gradually, unlike in the case of crystalline counterparts (where magnetization radically drops at T_C). Therefore it is more difficult to designate precisely the T_C in glassy samples. To solve this problem for the same $M(T)$ dependence as shown in Fig. 2 one can use the relation [12]:

$$M(T) = M_s(0)\left(1 - \frac{T}{T_C}\right)^{\beta}, \qquad (2)$$

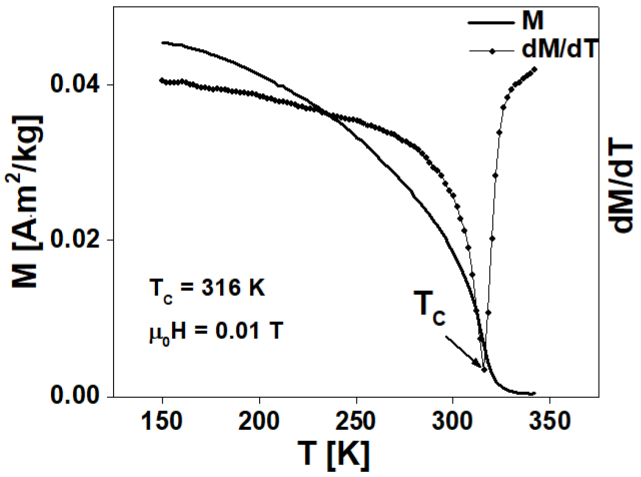

Fig. 2. Temperature dependence of magnetization $M(T)$ and its derivative dM/dT measured at $\mu_0 H = 0.01$ T for the $Gd_3Zr_{10}Fe_{55}Co_{10}Mo_5W_2B_{15}$ alloy ribbon.

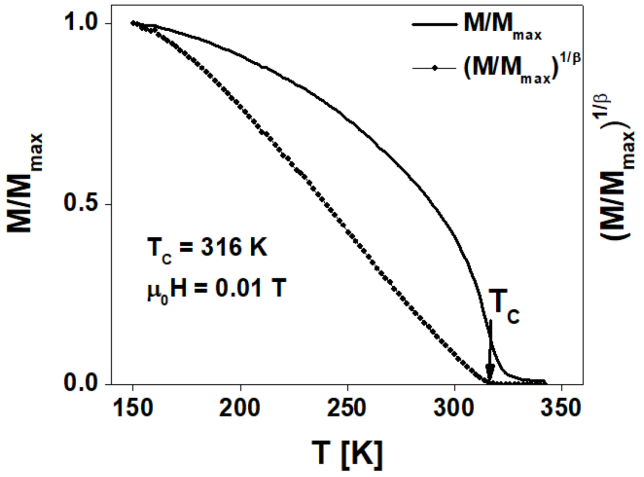

Fig. 3. The temperature T dependence of normalized magnetization $M/M_{\max}$ measured for the amorphous ribbon sample of the $Gd_3Zr_{10}Fe_{55}Co_{10}Mo_5W_2B_{15}$ alloy. Inset — the modified $(M/M_{\max})^{1/\beta}$ vs. T curve, where β is the critical parameter ($\beta = 0.365$) for the Heisenberg model.

where $M(T)$ is magnetization at temperature T, $M_S(0)$ is saturation magnetization at $T = 0$ K, and β is critical exponent which for the Heisenberg model is equal to 0.365 [13]. The temperature T dependence of the normalized magnetization $(M/M_{\max})^{1/\beta}$ calculated using the formula (2) and determination of $T_C = 316$ K were shown in Fig. 3.

3.3. Determination of the phase transition and T_C using Arrott plots

The magnetization curves were measured at various temperatures between 150 K and 340 K in external magnetic fields up to 7 T.

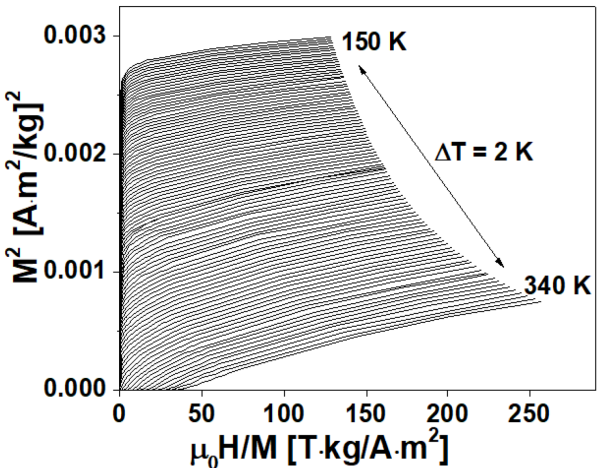

Fig. 4. Arrott plots, i.e. M^2 versus $\mu_0 H/M$ for the $Gd_3Zr_{10}Fe_{55}Co_{10}Mo_5W_2B_{15}$ glassy alloy in as-cast state.

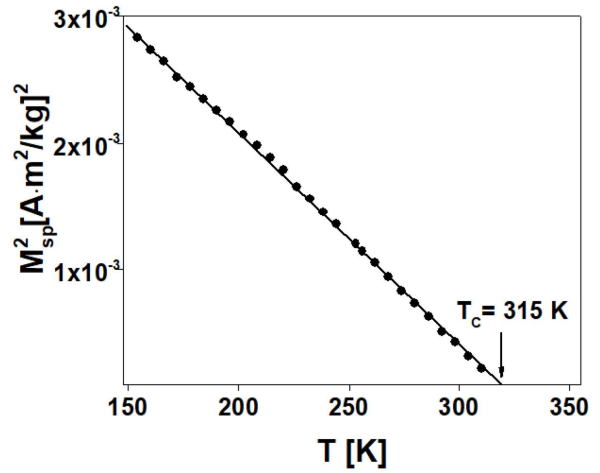

Fig. 5. Spontaneous magnetization M_{sp}^2 of $Gd_3Zr_{10}Fe_{55}Co_{10}Mo_5W_2B_{15}$ alloy ribbon vs. temperature T.

In order to determine the type of the magnetic phase transition and confirm T_C value obtained from previous measurements, the Arrott plots were constructed (Fig. 4).

The shapes of the Arrott plots are typical for alloys in which the second order phase transtion from ferro- to paramagnetic state around the Curie temperature takes place.

From $M^2(\mu_0 H/M)$ curves the relation M_{sp}^2 versus temperature T was constructed and T_C was determined. M_{sp}^2 values determined using extrapolations of the linear parts of M^2 vs. $\mu_0 H/M$ curves. Each M_{sp}^2 value was read as the interception of those extrapolations with M^2 axis (presented in Fig. 5).

The T_C calculated in this way reaches 315 K, which is in good agreement with the values obtained using two previously described methods.

3.4. Determination of T_C using $\mu_0 H(T)$ diagram

Another approach to verify T_C value was presented in Figs. 6–8. The magnetization isotherms $M(\mu_0 H)$ were cut across by constant magnetizations $M_i = M_1$, M_2, M_3, M_4, M_5, and M_6 (Fig. 6).

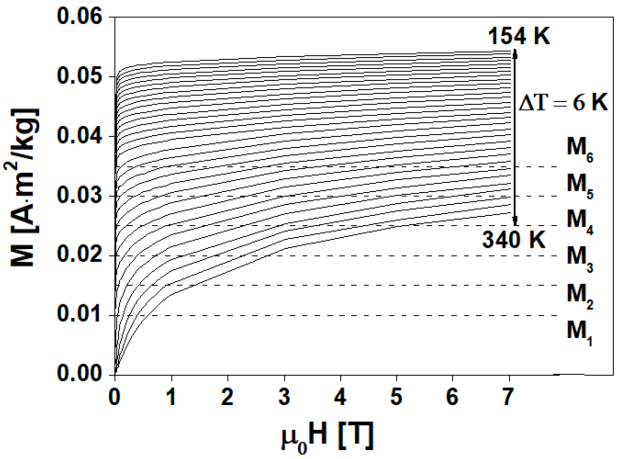

Fig. 6. The magnetic field $\mu_0 H$ dependences of magnetization M measured at various temperatures from 154 to 340 K ($\Delta T = 6$ K) for the amorphous ribbon of the $Gd_3Zr_{10}Fe_{55}Co_{10}Mo_5W_2B_{15}$ alloy.

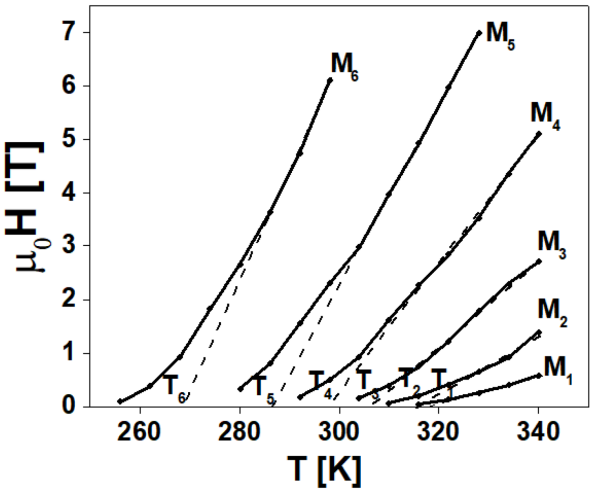

Fig. 7. $\mu_0 H(T)$ plot for the amorphous $Gd_3Zr_{10}Fe_{55}Co_{10}Mo_5W_2B_{15}$ alloy ribbon.

As a next step, the magnetic fields $\mu_0 H_{i,j}$ corresponding to the particular constant magnetizations M_i were read from $M(\mu_0 H)$ curves measured at various temperatures (from Fig. 6).

The temperature dependences of $\mu_0 H_{ij}$ corresponding to constant magnetizations M_i are presented in Fig. 7.

Subsequently the linear parts of $\mu_0 H(T)$ curves were linearly extrapolated to the zero magnetic fields and corresponding T_i temperatures were determined. Finally, the relation M_i vs. T_i was constructed and presented in Fig. 8.

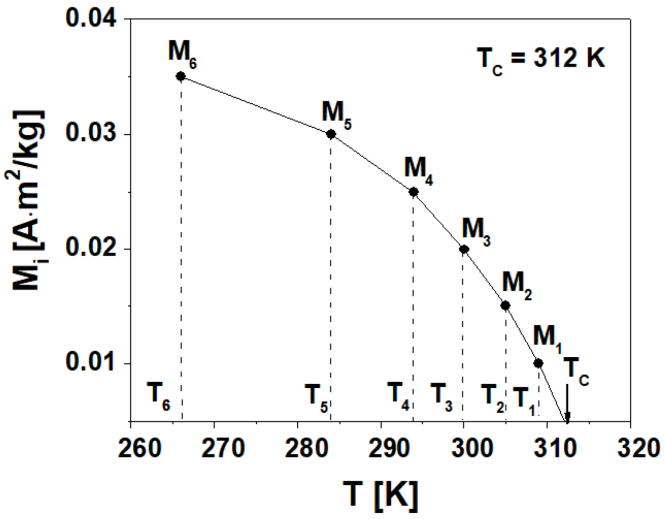

Fig. 8. M_i versus T_i for the amorphous $Gd_3Zr_{10}Fe_{55}Co_{10}Mo_5W_2B_{15}$ alloy ribbon.

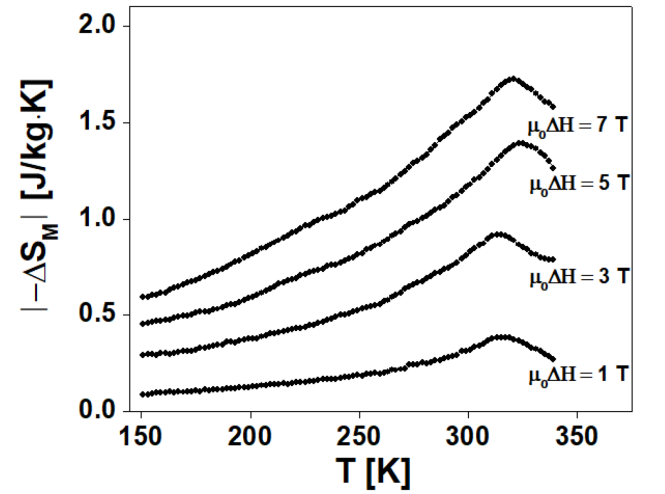

Fig. 9. Temperature dependence of the magnetic entropy changes $|-\Delta S_M|$ for the amorphous $Gd_3Zr_{10}Fe_{55}Co_{10}Mo_5W_2B_{15}$ alloy ribbon.

The Curie point was determined as an extrapolation of $M_i(T_i)$ curve to $M = 0$. The T_C value obtained using this method reached 312 K.

This value is slightly lower than those obtained by previous methods. However, it is more likely that twofold extrapolation used in this approach gives rise to potential systematic error.

3.5. Magnetocaloric effect

In order to assess the magnetocaloric effect in the investigated alloy the magnetic entropy change $|-\Delta S_M|$ vs. temperature T at various changes of magnetic fields were calculated using Eq. (1), based on measurement of $M(H)$ curves presented in Fig. 6. The temperature dependences of $|-\Delta S_M|$ were shown in Fig. 9. In all cases $|-\Delta S_M|$ reaches maximum around the Curie point. The maximum value of $|-\Delta S_M^{\max}|$ reached 1.75 J/(kg K) for the change of external magnetic field up to $\mu_0 H = 7$ T.

Based on our previous studies of the amorphous $Gd_xZr_{10}Fe_{58-x}Co_{10}Mo_5W_2B_{15}$ ($x = 0$, 1) alloy ribbons the increase of Gd contents to 3 at.% caused an increase of the Curie temperature without significant change of $|-\Delta S_M^{\max}|$.

4. Conclusion

The XRD studies of the melt-spun ribbon samples of the $Gd_3Zr_{10}Fe_{55}Co_{10}Mo_5W_2B_{15}$ alloy have shown their glassy structure. For this reason four different methods allowing to determine the Curie temperature, were used. All used methods have shown similar T_C values reaching 316 K. Relatively large T_C in comparison to the amorphous $Gd_xZr_{10}Fe_{58-x}Co_{10}Mo_5W_2B_{15}$ ($x = 0$, 1) alloy ribbons can be related to a higher Gd content in the studied sample. The tunable T_C around room temperature makes these alloys potentially useful for development of magentocaloric regenerators. Furthermore, construction of the Arrott plots confirmed a presence of second order phase transition around T_C.

Magnetic entropy change exhibits maximum at the Curie point (≈ 315 K) and reaches 1.75 J/(kg K) for the change of external magnetic field up to 7 T. Obtained values of $|-\Delta S_M|$ peaks for various changes of external magnetic fields are comparable to those obtained for the $Gd_xZr_{10}Fe_{58-x}Co_{10}Mo_5W_2B_{15}$ ($x = 0$, 1 alloy ribbons. Furthermore, wide bump of $|-\Delta S_M|$ vs. T suggests that the RCP should be large for the investigated alloy and seems to be promising for application.

References

[1] D. Vuarnoz, A. Kitanovski, C. Gonin, Y. Borgeaud, M. Delessert, P.W. Meinen, M. Egolf, *J. Appl. Eng.* **100**, 229 (2012).

[2] V. Chaudhary, D.V.D. Repaka, A. Chaturvedi, I. Sridhar, R.V. Ramanujan, *J. Appl. Phys.* **116**, 163918 (2014).

[3] P. Shamba, R. Zeng, J.L. Wang, S.J. Campbell, S.X. Dou, *J. Magn. Magn. Mater.* **331**, 102 (2013).

[4] A.O. Pecharsky, K.A. Gschneidner, V.K. Pecharsky, *J. Appl. Phys.* **93**, 4722 (2003).

[5] H. Wada, T. Asano, *J. Magn. Magn. Mater.* **290**, 703 (2005).

[6] H. Yibole, F. Guillou, L. Zhang, N.H.V. Dijk, E. Brück, *J. Phys. D Appl. Phys.* **47**, 1 (2014).

[7] K. Kotynia, P. Pawlik, M. Hasiak, *Hutnik Wiadomości Hutnicze* **84**, 425 (2017).

[8] K. Kotynia, P. Pawlik, A. Chrobak, in: *Works of XLV School of Material Engineering, Kraków–Rytro (Poland)*, 2017, p. 106.

[9] K. Kotynia, P. Pawlik, M. Hasiak, M. Pruba, K. Pawlik, *Acta Phys. Pol. A* **131**, 1204 (2017).

[10] K. Kotynia, A. Chrobak, P. Pawlik, in: *Works of XLVI School of Material Engineering, Kraków–Rytro (Poland)*, 2018, p. 85.

[11] K.A. Gschneidner, J.V.K. Pecharsky, *Ann. Rev. Mater. Sci.* **30**, 387 (2000).

[12] L. Banas, Z. Brzeźniak, M. Neklyudov, A. Prohl, in: *Stochastic Ferromagnetism*, Walter de Gruyter, 2014, p. 198.

[13] F. Ben Jemaa, S.H. Mahmood, M. Ellouze, E.K. Hlil, F. Halouani, *J. Mater. Sci.* **49**, 6883 (2014).